Fuzzy Generalized Hough Transform Invariant to Rotation and Scale in Noisy Environment

Hamid Izadinia, Fereshteh Sadeghi, Mohammad Mehdi Ebadzadeh, Member, IEEE

***Abstract*—Generalized Hough Transform (GHT) is an efficient method for detecting curves by exploiting the duality between points on a curve and parameters of that curve. However GHT has some practical limitations such as high computational cost and huge memory requirement for detecting scaled and rotated objects. In this paper a new method, namely Fuzzy Generalized Hough Transform (FGHT), is proposed that alleviates these deficiencies by utilizing the concept of fuzzy inference system. In FGHT the R-table consists of a set of fuzzy rules which are fired by the gradient direction of edge pixels and vote for the possible location of the center. Moreover, the proposed method can identify the boundary of the rotated and scaled object via a new voting strategy. To evaluate the effectiveness of FGHT several experiments with scaled, rotated, occluded and noisy images are conducted. The results are compared with two extensions of GHT and have revealed that the proposed method can locate and detect the prototype object with least error under various conditions.**

Keywords— Generalized hough transform, fuzzy inference system, object recognition, fuzzy voting.

I. INTRODUCTION

HOUGH Transform was initially developed to detect the analytically defined shapes such as lines, circles and ellipses in an image. The Generalized Hough Transform (GHT) was proposed by Ballard in order to detect instances of arbitrary complex shapes [1]. Although GHT is useful for shape analysis in occluded and noisy environments, it suffers from heavy computation and large memory requirement to handle the rotation and scale variations. More specifically, the conventional GHT takes a four dimensional space to recognize a known pattern which is rotated and scaled. Several methods such as [2]-[3] are proposed to reduce the memory requirements of GHT and are studied in [4]. The method proposed in [2] reduces the parameter space to two dimensions and constructs the R-table by pairs of edge points. In [3] the Point Spread Function (PSF) algorithm is adopted to handle the rotation and this method is extended in [4] to handle the scale variations.

Fuzzy Inference System (FIS) is a computational paradigm based on fuzzy set theory, fuzzy rules and fuzzy reasoning. The methods proposed in [5]-[9] apply the fuzzy concept to improve the performance of Hough Transform in noisy and blurred images, but these methods did not consider the rotation and scale variations.

In this paper a new extension of GHT, namely Fuzzy Generalized Hough Transform (FGHT), is proposed. FGHT employs the concept of fuzzy inference system in constructing the R-table. The R-table in FGHT consists of a set of fuzzy rules which fuzzifies the votes of edge pixels for the possible location of the center. Furthermore, the proposed method is equipped with a new voting strategy which estimates the angle of rotation and scaling factor of the test object to identify its boundary. In order to evaluate the performance of the proposed method several experiments on a set of rotated, scaled and occluded images in the presence and absence of noise are carried out.

This paper is organized as follows. Section II briefly reviews related methods. In Section III the Mamdani type of fuzzy inference system is presented. Section IV explains the details of the proposed method. Then, the experiments and obtained results are discussed in Section V. Finally, concluding remarks follow in Section VI.

II. RELATED WORKS

The proposed method is compared with two other extensions of GHT. Therefore, GHT along with its extensions are briefly reviewed in this section.

A. Generalized Hough Transform

In GHT [1], a line is drawn from a set of boundary points of the object to a reference point, usually the object centroid, as shown in Fig. 1 (a). A look-up table called R-table which is indexed by gradient of the boundary points (x_i, y_i) is constructed. The accumulator A is defined in the parameter space and saves the votes of the edge points to determine the most probable center of the prototype object in the test image. More specifically, the gradient angle β_j which is obtained from each edge point (u_j, v_j) is utilized to retrieve corresponding entries of the R-table. The possible location of reference point in the parameter space is calculated by the following equation.

$$(x_{cj}, x_{cj}) = \{u_j + r(\beta_j)\cos[\alpha(\beta_j)], v_j + r(\beta_j)\sin[\alpha(\beta_j)]\} \quad (1)$$

In the above equation, (x_{cj}, x_{cj}) stands for the location of the possible reference point. Also, $r(\beta_j)$ and $\alpha(\beta_j)$ denote the magnitude and the angle of the position vector retrieved from the R-table for index β_j, respectively.

The computational complexity of GHT is $(n_p/R_q)n_t S_q \theta_q$, where n_p and n_t are the number of edge pixels in the prototype object and test image, respectively. The parameters S_q and θ_q denote the resolution of the scale and the rotation parameter, respectively. Also, R_q stands for the

978-1-4244-3597-5/09/$25.00 ©2009 IEEE

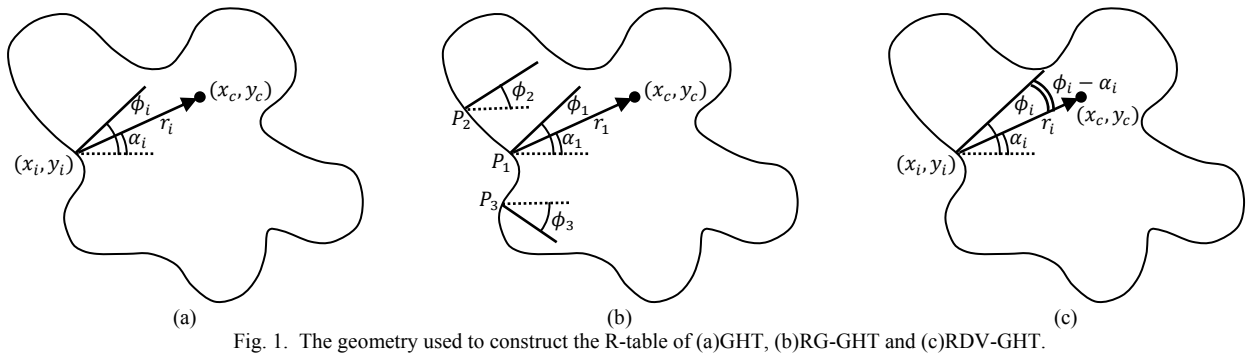

(a) (b) (c)

Fig. 1. The geometry used to construct the R-table of (a)GHT, (b)RG-GHT and (c)RDV-GHT.

resolution of the R-table index. GHT's memory requirement is $N^2 S_q \theta_q$, where N^2 is the size of the accumulator A. The major weakness of GHT is that the scale and rotation of the object is handled in a brute-force approach which requires a four-dimensional parameter space and high computational cost.

B. GHT using relative gradient angles (RG-GHT)

RG-GHT [2] is an orientation and scale-invariant method which reduces the parameter space to two dimensions. The R-table in this method is constructed by pairs of edge points as illustrated in Fig. 1 (b). The entries of the R-table are indexed by the difference between the gradient directions of the edge points P_1 and P_2 i.e. $\phi_2 - \phi_1$. Each entry of the R-table consists of the position vector, $R_1 = (r_1, \alpha_1)$, and the sum of the gradient directions of the same pair of edge pixels. The constructed R-table consists of the position vector, $R_1 = (r_1, \alpha_1)$, and the sum of the gradient directions of the edge points P_1 and P_3 i.e. $\phi_1 + \phi_3$. It should be noted that the separation between P_1', P_2' and P_3' of the test object has to be scaled by S which is obtained by the ratio of the perimeter of the test image to that of the prototype object.

Suppose that the difference between the gradient direction of P_1' and P_2' is equal to β. The corresponding entry of β in the R-table denotes the position vector of the possible reference point. The rotation angle of the test image θ_0 is calculated by eq. (2) and the position of the possible reference point is obtained from eq. (3).

$$\begin{aligned} &Angle\ of\ rotation \\ &= (gradient\ of P_1' + \ gradient\ of P_2' - \ (\phi_1 + \phi_3))/2 \\ &= ((\phi_1 + \theta_0) + (\phi_3 + \theta_0) - (\phi_1 + \phi_3))/2 = \theta_0 \end{aligned} \tag{2}$$

$$\begin{aligned} (x_{cj}, x_{cj}) = \{u_j + Sr(\beta_j)\cos[\alpha(\beta_j) + \theta_0], v_j \\ + Sr(\beta_j)\sin[\alpha(\beta_j) + \theta_0]\} \end{aligned} \tag{3}$$

RG-GHT can determine the boundary of the object by comparing the contour sequence of the object and that of the prototype. The computational cost of the detection stage in RG-GHT depends on the number of possible angles which is determined by the resolution of the rotation parameter θ_q.

The memory requirement of RG-GHT is N^2 and its computation complexity is $2n_t n_p / R_q$ wherein the factor of two accounts for pair of edge pixels.

C. GHT using relative displacement vectors (RDV-GHT)

The method proposed in [3] uses displacement vectors relative to the edge gradient direction in the R-table which makes it orientation invariant. In this method, instead of storing the angle of the position vector α_i, its difference to the gradient direction, i.e. $\phi_i - \alpha_i$, is saved in the R-table as depicted in Fig. 1 (c). In this method, the R-table, which consists of a set of relative displacement vectors $R_i = (r_i, \phi_i - \alpha_i)$, is adopted as a PSF. In other words, each edge pixel of the test image votes for the possible position of the center by all entries of the R-table. During shape detection, the position of the possible center is determined by the gradient direction β_j of each edge pixel (u_j, v_j) as follows:

$$\begin{aligned} (x_{cj}, x_{cj}) = \{u_j + r_i \cos[\beta_j - (\phi_i - \alpha_i)], v_j \\ + r_i \sin[\beta_j - (\phi_i - \alpha_i)]\} \end{aligned} \tag{4}$$

Although this method is rotation invariant, it is unable to handle scale variation. The RDV-GHT is an extension of [3] which handles the scale variation [4]. In RDV-GHT, lines corresponding to a range of defined scale are accumulated instead of accumulating points in the parameter space. The edge pixels vote for the possible center according to the eq. (5) in which the parameter *RS* is the range of scale that can be detected in the test image.

$$\begin{aligned} (x_{cj}, x_{cj}) = \{u_j + RSr_i \cos[\beta_j - (\phi_i - \alpha_i)], v_j \\ + RSr_i \sin[\beta_j - (\phi_i - \alpha_i)]\} \end{aligned} \tag{5}$$

The memory requirement of RDV-GHT is N^2 and its computation complexity is $n_t n_p k \bar{r}(S_u - S_l)$ where S_u and S_l are the upper and lower limits of the scale, respectively. Also, the average magnitude of the edge position vectors is $\bar{r}$ and the factor $k \leq 1$ is included because the voting procedure is limited by the size of the parameter space.

III. FUZZY INFERENCE SYSTEM

Fuzzy Inference Systems (FIS) are based on the concept of fuzzy set theory and due to their closeness to human perception and their simplicity have been applied with success in many fields [10]. Fig. 2 illustrates the general schema of a FIS which consists of three major components called fuzzifier, rule base and defuzzifier. The fuzzifier and the defuzzifier convert crisp information to fuzzy quantities and vice versa. The reasoning of FIS takes place in the rule

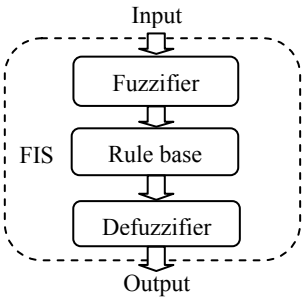

Fig. 2. The scheme of a Fuzzy Inference System.

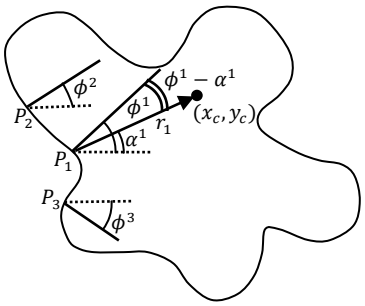

Fig. 3. The geometry used to construct the R-table of FGHT.

base which is composed of a collection of fuzzy rules. The need for fuzzifier or defuzzifier will be eliminated whenever fuzzy input data are available or the fuzzy output is desired.

Typically, a FIS can be classified according to three types of models that are distinguished in the formalization of the fuzzy rules [11]. In this paper, the Mamdani type [12] which is expressed by the fuzzy rule schema of eq. (6) is employed.

$$\textit{if } \boldsymbol{x} \textit{ is } \boldsymbol{A} \textit{ then } \boldsymbol{y} \textit{ is } \boldsymbol{B} \tag{6}$$

In the above equation, A and B denote the fuzzy sets defined on the input and output domains, respectively. The Mamdani FIS is a nonlinear mapping from an input domain $X \epsilon \mathbb{R}^n$ to an output domain $Y \epsilon \mathbb{R}^m$. This mapping contains R rules of the following form:

$$\textit{if } \boldsymbol{x} \textit{ is } \boldsymbol{A}_r \textit{ then } \boldsymbol{y} \textit{ is } \boldsymbol{B}_r \tag{7}$$

where $r = 1,2,\dots,R$ is the index of the rule. Suppose an input vector x is presented to the system, a fuzzy set B is inferred by

$$B(y) = \bigvee_{r=1}^{R} (A_r(x) \wedge B_r(y)) \tag{8}$$

in which the $A(.)$ denotes the membership function of a fuzzy set A. Also, $\wedge$ and $\vee$ are a T-norm and a T-conorm, respectively. When a crisp output is required, several different strategies may be utilized for defuzzifing the resulting fuzzy set to a crisp value.

IV. Proposed Method

In this section, an extension of generalized hough transform using fuzzy inference system is proposed. The proposed method is invariant to the scale and rotation changes even in occluded and noisy images. FGHT finds the center of object as well as the object itself without noticeable computational overhead. In FGHT, the R-table is constructed based on the geometry presented in Fig. 3. The proposed method employs the R-table as a FIS wherein each row contains the antecedent and the consequence parts of a fuzzy rule. The antecedent and consequence parts of each fuzzy rule are based on the gradient direction at the edge pixel rather than the axes of the image space. This modification in R-table makes the FGHT invariant to the object rotation. As opposed to the GHT where each edge pixel votes for a crisp reference point, in the FGHT an area around the possible reference point is voted by a single edge pixel. This area is determined based on the fuzzy set in the consequence part of the fired fuzzy rule.

The antecedent part of each fuzzy rule contains two fuzzy sets each of which is determined by the difference of gradient direction between a pair of edge pixels. Fig. 3 illustrates how the centers of fuzzy sets are determined in an edge pixel (P_1). The center of the first fuzzy set is determined by the difference between the gradient direction of P_1 and P_2 i.e. $\phi^2 - \phi^1$. Likewise, the center of the second fuzzy set is determined by the difference between the gradient direction of P_3 and P_1 i.e. $\phi^1 - \phi^3$. The consequence part consists of two fuzzy sets whose centers for the instance point P_1 are set by the magnitude of position vector (r_1) and relative angle between position vector and gradient direction ($\phi^1 - \alpha^1$). The ith fuzzy rule in R-table corresponding to the edge pixel P_1 of the prototype image which is illustrated in Fig. 3 is defined by (9).

$$\begin{aligned} &\delta_i^1 = \phi_i^2 - \phi_i^1 \\ &\delta_i^2 = \phi_i^1 - \phi_i^3 \\ &\textit{if } \delta_j^1 \textit{ is } \delta_i^1 \textit{ and } \delta_j^2 \textit{ is } \delta_i^2 \Rightarrow r_j \textit{ is } \Re_i \textit{ and } \theta_j \textit{ is } \Theta_i \end{aligned} \tag{9}$$

In the above equation, δ_j^1 is the difference between the gradient direction of edge pixel P_1' in the test image and the next edge pixel with specific distance (P_2'). Also, δ_j^2 is the difference between the gradient direction of P_1' and previous edge pixel (P_3') in the test image. The fuzzy sets corresponding to δ_j^1 and δ_j^2 are δ_i^1 and δ_i^2, respectively. In the consequence part of the fuzzy rule, the r_j is the magnitude of the possible position vector and the θ_j is the relative angle between possible position vector and gradient direction of P_1' i.e. $\theta_j = \phi_j^1 - \alpha_j^1$. The fuzzy sets in ith fuzzy rule corresponding to r_j and θ_j are denoted by $\Re_i = \left(c_{\Re_i}, \sigma_{\Re_i}\right)$ and $\Theta_i = \left(c_{\Theta_i}, \sigma_{\Theta_i}\right)$, respectively. The fuzzy sets in FGHT are represented by Gaussian membership functions with specific center c and width σ.

The voting process for the possible center in FGHT is based on the fuzzy concept. The output of each fuzzy rule in the R-table for an edge pixel of the test image is determined by the production of the corresponding fuzzy sets in consequence part and is weighted by its firing strength. The firing strength of a fuzzy rule is the degree to which the antecedent part of a fuzzy rule is satisfied. In FGHT, the set

of possible centers of the object for *j*th edge pixel in the test image (u_j, v_j) is defined by eq. (10). The membership of each element of $\{(x_{cj}, y_{cj})\}$ is determined by eq. (11) and is considered as a fuzzy vote of the *j*th edge pixel for the possible center. The corresponding position of the *A* accumulator is updated via eq. (12).

$$\{(x_{cj}, y_{cj})\} = \{(u_j + r_i^k \cos(\phi_j - \theta_i^k), v_j + r_i^k \sin(\phi_j - \theta_i^k)) | r_i^k \in \Re_i, \theta_i^k \in \Theta_i\} \quad (10)$$

$$\mu(x_{cj}, y_{cj}) = \mu_{\delta_i^1}(\delta_j^1) * \mu_{\delta_i^2}(\delta_j^2) * \mu_{\Re_i}(r_i^k) * \mu_{\Theta_i}(\theta_i^k) \quad (11)$$

$$A[x_{cj}][y_{cj}] = A[x_{cj}][y_{cj}] + \mu(x_{cj}, y_{cj}) \quad (12)$$

FGHT can obtain the rotation and scale of the object as well as determining its center. To do so, edge pixels vote for the possible values of rotation and scale. Finally the angle of rotation and the scaling factor which have gained the majority of votes are considered as the most probable angle of rotation and scale of the object.

In the training phase, the gradient direction at each edge pixel of the prototype image is saved for the entries of the R-table. The votes of the rotation angle are saved in an array named rotation accumulator (*RA*). The length of *RA* is determined according to the resolution of rotation. The *RA* is updated by the votes of the *j*th edge pixels for the possible angle according to eq. (13)-(15).

$$\xi_j = round(\psi_j - \phi_i) \quad (13)$$

$$\mu(\xi_j) = \mu_{\delta_i^1}(\delta_j^1) * \mu_{\delta_i^2}(\delta_j^2) \quad (14)$$

$$RA[\xi_j] = RA[\xi_j] + \mu(\xi_j) \quad (15)$$

In the above equations, ψ_j stands for the gradient direction at the *j*th edge pixel of the test image and $round(.)$ rounds the estimated rotation angle to the nearest value in the rotation resolution. It should be noted that the estimation of rotation angle and detection of the object's center are performed simultaneously.

Once the rotation angle and center of the object are determined, the scale of the object will be estimated. Similar to the rotation estimation an array named scale accumulator (*SA*) with the resolution of scaling factor is utilized. For each entry of the R-table the scaling factor *S* varies from minimum to maximum value and the edge pixel corresponding to this entry is obtained by the eq. (16). In this paper *S* varies from 0.5 to 2.

$$(x_i, y_i) = \{x_c - Sr_i \cos(\alpha_i + \xi_0), y_c - Sr_i \sin(\alpha_i + \xi_0)\} \quad (16)$$

In this equation, (x_c, y_c) and ξ_0 denote the center and the rotation angle of the object which is obtained from the previous step. If (x_i, y_i) in the test image is an edge pixel, the corresponding scaling factor in *SA* is incremented according to the eq. (17).

$$SA[S^*] = SA[S^*] + 1 \quad (17)$$

The memory requirement of the FGHT is equal to the sum of the size of *A*, *RA* and *SA* i.e. $N^2 + S_q + \theta_q$. The computational complexity of the FGHT is determined by the number of updates in the accumulator. The number of updates depends on the width of the fuzzy sets in the consequence part of the fuzzy rules. Because the updating process is performed from $-\sigma_{\Re_i}$ to $+\sigma_{\Re_i}$ and from $-\sigma_{\Theta_i}$ to $+\sigma_{\Theta_i}$, the computational complexity of FGHT is proportional to $4\sigma_{\Re_i}\sigma_{\Theta_i}$ and is equal to $2(n_p/R_q)n_t k(4\bar{\sigma}_{\Re}\bar{\sigma}_{\Theta})$.

V. Experiments and Results

In this section the performance of the proposed method is evaluated by several experiments under the following conditions: scale and rotation variation, occlusion and in the presence of noise. The binary image of a car depicted in Fig. 4 (a) is used as the prototype object. The test images used in the experiments include copies of the prototype object in different scales, angles of rotation, and occluded with a tree in the absence and presence of noise which are illustrated in Fig. 4 (b)-(g). The FGHT parameter setting that is common for all experiments is presented in TABLE I. The results of FGHT are compared with that of RG-GHT and RDV-GHT with respect to the localization and detection errors which are defined by eq. (18) and (19).

TABLE I
Fuzzy set parameters in FGHT

fuzzy set	membership functions	
	center(c)	width(σ)
δ_i^1	$\phi_i^2 - \phi_i^1$	5
δ_i^2	$\phi_i^1 - \phi_i^3$	5
$\Re_i$	r_i	$0.9r_i$
Θ_i	$\phi_i^1 - \alpha_i^1$	5

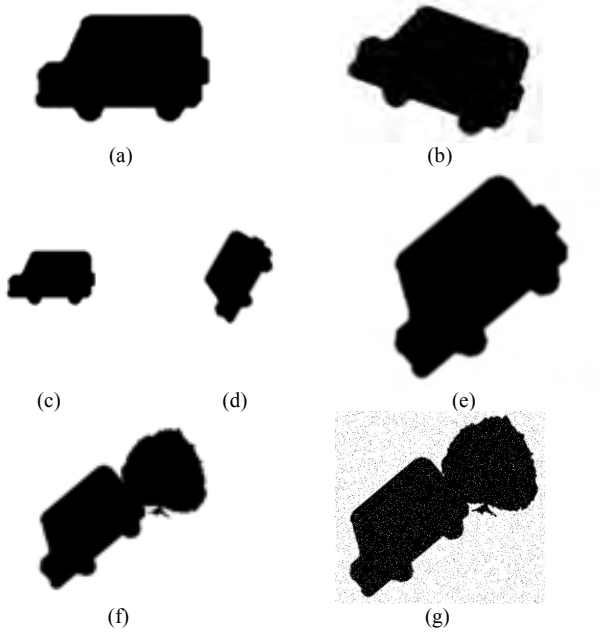

Fig. 4. The prototype and test images. (a)prototype object, the test images with (b)scale=1 and rotation=20°; (c)scale=0.5 and rotation=0°; (d)scale=0.5 and rotation=−60°; (e)scale=1.2 and rotation=−40°; (f)scale=0.8, rotation=−40° and occlusion; (g)scale=0.8, rotation=−40°, occlusion with impulse noise(5%);

$$E_l = \sqrt{(x_c - x_c')^2 + (y_c - y_c')^2} \quad (18)$$

$$E_d = \frac{1}{R_q}\sum_{i=0}^{R_q} D(P_i, P_i') \quad (19)$$

The (x_c, y_c) and (x_c', y_c') in eq. (18) denote the actual and estimated center of the object, respectively. In eq. (19), R_q stands for the number of entries in the R-table which corresponds to the number of sample points of the prototype object and $D(.,.)$ is the Euclidian distance function. Also, P_i and P_i' are the edge pixel of the prototype object in the test image and the detected object, respectively. It should be noted that the RDV-GHT does not have the capability of detecting the boundary of the test object. Therefore, the detection error is only computed for FGHT and RG-GHT.

The experiments are conducted in two parts. In the first part, the performance of the proposed method is assessed in case of rotation and scale variation and the results are summarized in TABLE II. In the second part, a complicated image is tested. In this image the prototype object not only is rotated and scaled but also is occluded by a tree. This image is tested in the absence and presence of impulse noise. The results of the second part of experiments are presented in TABLE III. In the results of TABLE II and TABLE III, other than localization and detection errors, the position, size and the offset of the peak are presented for each experiment. The size of the peak refers to the amount of vote for the possible center and the offset is the separation between the peak and the centroid of the prototype object in the test image which provides a measure of the accuracy of the methods.

The antecedent and consequence parts of the fuzzy rules in FGHT are independent of the image space. This is due to the use of the difference between the gradient direction in the pair of edge pixels in the antecedent part and the relative angle between the position vector and the gradient direction in the consequence part. Therefore, the proposed method is invariant to the rotation of the prototype object.

Compared with RG-GHT and RDV-GHT, FGHT performs more efficiently under the rotation. The RG-GHT estimates the curvature by utilizing the difference between the gradient directions of a pair of edge pixels so that it can handle the rotation variations. The proposed method strengthens this idea by employing two pairs of points. Hence, FGHT can handle rotation more efficiently if the contour of the object is distorted. Moreover, RDV-GHT adopts the R-table as a PSF so that all entries of the R-table are utilized in the voting process that may generate false peaks in the accumulator. FGHT eliminates this problem by employing the R-table as a FIS in which the output of each rule is weighted by its firing strength.

From the point of view of scale variation handling, the RG-GHT has poor performance. Because it estimates the scaling factor by calculating the ratio of the perimeter of the test image and that of the prototype thereby it will fail in the occluded and noisy images. Although RDV-GHT can handle scale variations acceptably, it leads to false peaks near the actual peak due to voting through a line with the same quantity. On the other hand, instead of voting for a single center, the FGHT votes for a set of probable centers via the fuzzy sets which correspond to the magnitude of the position vectors in the consequence part of the fuzzy rules. In other words, FGHT votes for the most probable center with greater quantities rather than the neighboring least probable pixels so that it can handle the scale variation without producing false peaks.

TABLE II summarizes the results of FGHT compared with the RG-GHT and RDV-GHT at scales of 1.0, 0.5 and 1.2 and rotational angle of $20^\circ, 0^\circ, -60^\circ$ and -40° .The results show that in all cases the proposed method has identified the location of the object with smallest offset and hence least localization error.

As mentioned before, the RG-GHT fails in noisy and occluded environments. RDV-GHT can handle occlusion effectively but have poor performance under the noise so it fails to recognize the prototype object in the test image of Fig. 4 (g). the state of the accumulator *A* after applying RDV-GHT and FGHT on the test image of Fig. 4 (g) is shown in Fig. 5. According to Fig. 5, RDV-GHT produces a false peak near the centroid of the tree at [465,185] whereas FGHT does not produce any false peak and has a small localization error.

FGHT can tolerate noise efficiently owing to the use of fuzzy sets in both the antecedent and consequence parts of the fuzzy rules. The results of TABLE III reveal that FGHT performs very well in the complex test image with rotation, scale and occlusion. In addition to that the results obtained from the same image in the presence of noise are quite the

TABLE II
Comparison of FGHT with RG-GHT and RDV-GHT

scale	rotation	Method	peak position	peak size	offset	localization error	detection error
1.0	20°	FGHT	[312,274]	96.58	**[-2,-4]**	**4.47**	**1.22**
		RG-GHT	[300,265]	41	[10,5]	11.18	3.99
		RDV-GHT	[308,269]	196	[6,2]	6.32	-
0.5	0°	FGHT	[133,96]	111.22	**[-4,0]**	**4**	**1.04**
		RG-GHT	[123,97]	56	[6,-1]	6.08	1.5
		RDV-GHT	[133,101]	108	[-4,-5]	6.4	-
0.5	-60°	FGHT	[149,164]	22.83	**[-1,-2]**	**2.24**	**0**
		RG-GHT	[147,166]	30	[1,-4]	4.12	0.42
		RDV-GHT	[148,162]	102	[-1,-5]	5.1	-
1.2	-40°	FGHT	[383,384]	160.41	**[5,-4]**	**6.4**	**1.38**
		RG-GHT	[380,389]	187	[8,-9]	12.04	2.14
		RDV-GHT	[378,366]	201	[10,14]	17.2	-

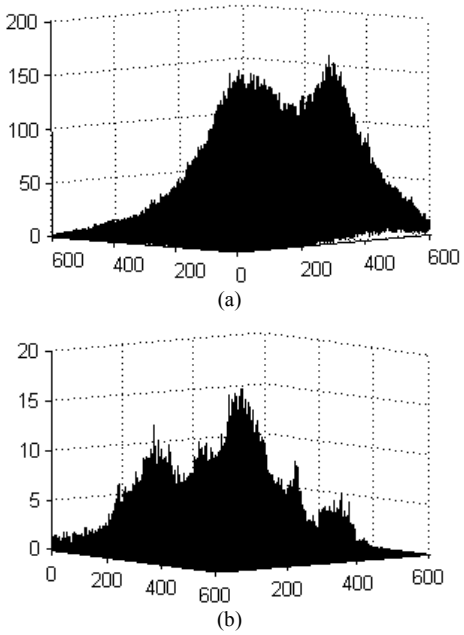

Fig. 5. The parameter space of (a)RDV-GHT and (b)FGHT.

same as the non-noisy version. This proves our claim that the FGHT is robust under the noisy conditions.

The final state of *RA* and *SA* after the experiment corresponding to Fig. 4 (f) is illustrated in Fig. 6 (a) and (b), respectively. According to Fig. 6 (a) there is a peak at the value of 0.8 in the *SA* which denotes the estimated scaling factor. The peak in *SA* is quite distinguishable which means that FGHT can determine the scaling factor effectively. The peak at the value of -40° of the *RA* array in Fig. 6 (b) shows the estimated rotation angle. Another peak at the value of 140° is also generated by the FGHT. This is due to the parallel lines in the prototype object with the same curvature whose difference of gradient direction is 180°. If there are several peaks without considerable difference with the maximum value, the rotation angle is determined by testing each of them. It is worth mentioning that as opposed to RG-GHT which determines the rotation angle and scaling factor via a search in all the possible rotation angles, the proposed method can identify them without extra computation.

VI. Conclusion

In this paper the GHT is extended by employing the fuzzy concept in constructing the R-table and is named Fuzzy Generalized Hough Transform (FGHT). The new method has advantages over the GHT in that it can perform very well in the scaled, rotated and occluded objects even in the presence of noise. In FGHT the R-table is utilized as a FIS and the possible center of the object is determined based on the fuzzy votes of the edge pixels. Moreover, FGHT can identify the boundary of the rotated or scaled object accurately by means of a new voting strategy. To assess the performance of the FGHT several experiments are conducted and the results are compared with the results of RG-GHT and RDV-GHT. The results show that the proposed method is more accurate in localizing the center of the prototype object as well as detecting the boundary of the test object with the least error.

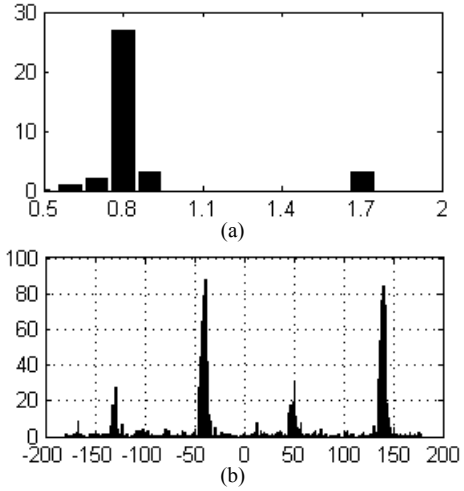

Fig. 6. The accumulator (a)SA and (b)RA.

TABLE III
Comparison of FGHT with RG-GHT and RDV-GHT

method	peak position	peak size	offset	localization error	detection error
FGHT	[297,301]	77.94	**[-3,0]**	**3**	**2.77**
RG-GHT	[209,236]	98	[164,15]	164.68	62.51
RDV-GHT	[299,296]	174	[-5,5]	7.07	-
FGHT	[293,300]	16.06	**[1,1]**	**1.41**	**3.18**
RG-GHT	[196,145]	91	[98,156]	184.23	42.19
RDV-GHT	[465,185]	164	[-171,116]	206.63	-

References

[1] D. H. Ballard, "Generalizing the Hough transform to Detect Arbitrary Shapes," *Pattern Recognition*, vol. 13, pp. 111-122, 1981.

[2] P. -K. Ser, and W. -C. Siu, "Non-analytic object recognition using the Hough transform with the matching technique," Computers and Digital Techniques, IEE Proceedings, vol.141, no.1, pp.11-16, 1994.

[3] A. D. H. Thomas, "Compressing the parameter space of the generalised Hough transform," Hough Transforms, IEE Colloquium on, pp. P1/1- P1/4, 1993.

[4] A. A. Kassim, T. Tan, and K. H. Tan, "A comparative study of efficient generalized Hough transform techniques," *Image Vis. Comput.*, vol. 17, no. 10, pp. 737-748, 1999.

[5] N. Suetake, E. Uchino, and K. Hirata, "Generalized fuzzy Hough transform for detecting arbitrary shapes in a vague and noisy images," *Soft Computing - A Fusion of Foundations, Methodologies and Applications*, vol. 10, no. 12, pp. 1161-1168, 2006.

[6] J. Basak, and S. K. Pal, "Theoretical quantification of shape distortion in fuzzy Hough transform," *Fuzzy Sets and Systems*, vol. 154, pp. 227–250, 2005.

[7] K. P. Philip, E. L. Dove, D. D. McPherson, N. L. Gotteiner, W. Stanford, K. B. Chandran, "The fuzzy Hough transform-feature extraction in medical images," *Medical Imaging, IEEE Transactions on*, vol.13, no.2, pp.235-240, 1994.

[8] J. H. Han, L. T. Koczy, and T. Poston, "Fuzzy Hough transform," Fuzzy Systems, 1993, *Second IEEE International Conference on* , vol. 2, pp. 803-808.

[9] R. Soodamani, and Z. Q. Liu, "A novel fuzzy Hough transform for shape representation," *Fuzzy Systems Proceedings*, 1998, vol. 2, pp. 1605-1608.

[10] T. J. Ross, *Fuzzy Logic with Engineering Applications*, New York: McGraw-Hill, 1995.

[11] J. -S. R. Jang, and C. T. Sun, "Neuro-fuzzy modeling and control," *Proceedings of the IEEE* , vol.83, no.3, pp.378-406, Mar 1995

[12] E. H. Mamdani, and S. Asilian, "An experiment in linguistic sysnthesis with a fuzzy logic controller," *International Journal of Man-Machine Studies*, 7(1), 1-13, 1975.